© 2024 Journal of Pharmacy & Pharmacognosy Research, 12 (2), 231-242, 2024
ISSN 0719-4250
https://jppres.com

DOI: https://doi.org/10.56499/jppres23.1743_12.2.231

Original Article

Synthesis and evaluation of a rociletinib analog as prospective imaging double mutation L858R/T790M in non-small cell lung cancer

[Síntesis y evaluación de un análogo de rociletinib como imagen prospectiva de la doble mutación L858R/T790M en cáncer de pulmón no microcítico]

Muammar Fawwaz[1,2*], Kenji Mishiro[3], Bambang Purwono[4***], Ryuichi Nishii[5], Kazuma Ogawa[2,3]**

[1]Faculty of Pharmacy, Universitas Muslim Indonesia, Urip Sumoharjo KM. 5, Makassar 90-231, Indonesia.
[2]Graduate School of Medical Sciences, Kanazawa University, Kakuma-machi, Kanazawa, Ishikawa 920-1192, Japan.
[3]Institute for Frontier Science Initiative, Kanazawa University, Kakuma-machi, Kanazawa, Ishikawa 920-1192, Japan.
[4]Laboratory of Organic Chemistry, Faculty of Mathematics and Natural Sciences, Universitas Gadjah Mada, Yogyakarta, Indonesia.
[5]Biomedical Imaging Sciences, Department of Integrated Health Sciences, Graduate School of Medicine, Nagoya University, Japan.
*E-mail: *muammar.fawwaz@umi.ac.id; **mishiro@p.kanazawa-u.ac.jp; ***purwono.bambang@ugm.ac.id

Abstract

Context: Imaging the mutation status of non-small cell lung cancer (NSCLC) using radiolabeled tyrosine kinase inhibitor (TKI) analogs has garnered interest due to their unique interactions with the target epidermal growth factor receptor (EGFR). Rociletinib is a third-generation TKI that selectively inhibits the activated EGFR L858R/T790M mutations while sparing the wild-type EGFR.

Aims: To synthesize a rociletinib analog for radioiodination purposes and evaluate its affinity for EGFR L858R/T790M using molecular docking and *in vitro* cytotoxicity assay.

Methods: The rociletinib analog, *N*-{3-[(4-{[4-(4-acetylpiperazin-1-yl)-2-methoxyphenyl]amino}-5-(trifluoromethyl)pyrimidine-2-yl)amino] -5-iodophenyl} acrylamide (I-RMFZ), was produced by adding iodine into the diaminophenyl group and changing the position of the trifluoromethyl group. A simulation of molecular docking was conducted using the AutoDock Vina software suite. IC_{50} of I-RMFZ was determined using a cell cytotoxicity assay.

Results: I-RMFZ was successfully synthesized through multistep reactions. Molecular docking revealed that I-RMFZ interacts with the EGFR L858R/T790M mutation. Cytotoxicity assay demonstrated that I-RMFZ had a high selectivity towards EGFR L858R/T779M mutation.

Conclusions: I-RMFZ is notable for radioiodination and is anticipated to be comparable with *in vivo* features of rociletinib. Thus, I-RMFZ can potentially be developed as an imaging agent for NSCLC through preclinical assay.

Keywords: acrylamide; carcinoma; epidermal growth factor; molecular docking simulation; mutation.

Resumen

Contexto: La obtención de imágenes del estado de la mutación del cáncer de pulmón no microcítico (CPNM) utilizando análogos radiomarcados de inhibidores de la tirosina cinasa (TKI) ha despertado interés debido a sus interacciones únicas con el receptor del factor de crecimiento epidérmico (EGFR) diana. El rociletinib es un TKI de tercera generación que inhibe selectivamente las mutaciones activadas L858R/T790M del EGFR, mientras que no afecta al EGFR de tipo salvaje.

Objetivos: Sintetizar un análogo de rociletinib con fines de radioiodinación y evaluar su afinidad por EGFR L858R/T790M mediante acoplamiento molecular y ensayo de citotoxicidad *in vitro*.

Métodos: El análogo de rociletinib, N-{3-[(4-{[4-(4-acetilpiperazin-1-il)-2-metoxifenil]amino}-5-(trifluorometil)pirimidin-2-il)amino] -5-yodofenil}acrilamida (I-RMFZ), se produjo añadiendo yodo al grupo diaminofenil y cambiando la posición del grupo trifluorometil. Se realizó una simulación de acoplamiento molecular utilizando el paquete de software AutoDock Vina. El IC_{50} de I-RMFZ se determinó mediante un ensayo de citotoxicidad celular.

Resultados: I-RMFZ se sintetizó con éxito mediante reacciones de múltiples pasos. El acoplamiento molecular reveló que I-RMFZ interacciona con la mutación L858R/T790M del EGFR. El ensayo de citotoxicidad demostró que I-RMFZ tenía una alta selectividad hacia la mutación L858R/T779M del EGFR.

Conclusiones: I-RMFZ destaca por su radioiodinación y se prevé que sea comparable con las características *in vivo* de rociletinib. Así pues, I-RMFZ puede desarrollarse potencialmente como agente de imagen para CPNM mediante ensayo preclínico.

Palabras Clave: acrilamida; carcinoma; factor de crecimiento epidérmico; simulación de acoplamiento molecular; mutación.

ARTICLE INFO
Received: July 15, 2023.
Accepted: November 10, 2023.
Available Online: December 15, 2023.

AUTHOR INFO
ORCID: 0000-0002-6046-2819 (MF)
0000-0002-5071-7574 (KM)
0000-0002-1691-7302 (KO)

INTRODUCTION

The human epidermal growth factor receptor (EGFR) is one of the four receptor tyrosine kinases in the EGFR family (Yarden and Sliwkowski, 2001). The EGFR is a transmembrane glycoprotein with 1186 amino acids. It has an extracellular, a transmembrane, and an intracellular tyrosine kinase domain. EGFR is involved in several cellular processes, such as cell growth, division, differentiation, and death (Yarden, 2001). Moreover, it is also over-expressed in several human cancers, such as those of the lung, breast, head, neck, colon, and rectum (Hirsch et al., 2003; Walker and Dearing, 1999).

EGFR tyrosine kinase inhibitors (TKIs), such as gefitinib and erlotinib, have been widely investigated as potent EGFR-targeted drugs. The application of these TKIs in patients with a single-site mutation of non-small cell lung cancer (NSCLC) has been extensively reviewed (Park et al., 2021; Singh and Jadhav, 2018). This class of drugs can specifically bind to the intraendothelial TK domain of EGFR, thereby suppressing tumor growth by blocking signaling pathways (Yan et al., 2017). Therefore, using these drugs to treat patients with NSCLC is considered adequate (Ariyama et al., 2021). However, after 9–14 months of the treatment, EGFR mutation-positive patients typically develop drug resistance, and their tumors grow. In 50-60% of the recurrent cases, drug resistance is caused by a secondary point mutation in EGFR, which results in a threonine-to-methionine change at position 790 (T790M) (Kosaka et al., 2006; Sequist et al., 2011; Yan et al., 2017).

To effectively treat NSCLC patients with double mutation EGFR, identifying the mutation status of NSCLC is necessary. Biopsy is the most commonly used method for determining the mutation status of NSCLC. Further, cancer tissues are known to be heterogeneous (Lüönd et al., 2021; Xu et al., 2021), and a biopsy can only provide limited information on the entire cancer tissue (Xiao et al., 2017). Moreover, patients must be burdened by recurrent intrusive biopsies (Hirsch et al., 2005). Therefore, a more effective method, such as diagnostic imaging, is required.

Several radioactive imaging agents with positron emission tomography (PET) or single-photon emission computed tomography (SPECT) play a crucial role in precision medicine (Manning, 2015; Waaijer et al., 2018). Furthermore, nuclear medicine imaging is noninvasive and can reveal quantitative details of *in vivo* biological activities with excellent sensitivity. In response to the restrictions of an intrusive biopsy and any bias originating from the heterogeneity of the tumor (Peled et al., 2017; Tan et al., 2016), molecular imaging employing PET or SPECT can stratify patients based on their susceptibilities to various diseases and may be classified into the genetic, molecular, or cellular profiles (Sun et al., 2018).

Certain imaging probes for TKIs have been developed to determine the EGFR mutation status in NSCLC. However, the radiotracers used to image EGFR L858R/T790M double mutations, such as [^{11}C]osimertinib, [^{11}C]rociletinib, [^{125}I]ICO1686, [^{77}Br]BrCO1686, [^{125}I]I-osimertinib, and [^{77}Br]Br-osimertinib, have certain limitations (Fawwaz et al., 2023). These radiotracers do not predominately accumulate in the targeted tumor, thereby resulting in a low tumor-to-blood ratio (Ballard et al., 2016; Fawwaz et al., 2020; 2021; Mishiro et al., 2022).

Rociletinib (Fig. 1) is one of the orally active third-generation TKIs that selectively inhibits activated EGFR with L858R/T790M double mutations in NSCLC. The chemical structure of rociletinib contains crucial functional groups, namely the pyrimidine and trifluoromethyl groups. Both groups play a crucial role in facilitating the binding of rociletinib to the ATP binding site of EGFR L858R/T790M (Yan et al., 2017). Rociletinib can be developed as an imaging agent for dual mutations NSCLC owing to its specific affinity to EGFR L858R/T790M.

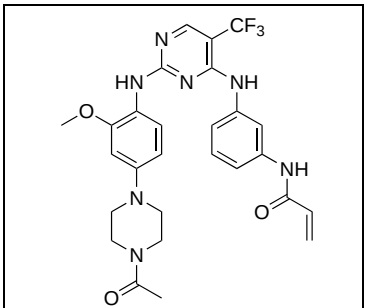

Figure 1. The structure of rociletinib.

Owing to the availability of numerous radioiodine isotopes, including ^{123}I with a half-life ($t_{1/2}$) of 13.2 h for SPECT imaging, ^{131}I with a $t_{1/2}$ of 8.0 d for radionuclide therapy, and ^{124}I with a $t_{1/2}$ of 4.2 d for PET imaging, as well as ^{125}I for various preclinical studies (Cavina et al., 2017; Dubost et al., 2020; Ogawa et al., 2009; 2018; Patel et al., 2015), we previously developed a novel radioiodinated analog of rociletinib by introducing iodine in the diaminophenyl group (Fawwaz et al., 2020). In this study, we found that an iodinated rociletinib isomer can be easily synthesized from a side product obtained during the synthesis of an iodinated rociletinib. Moreover, a docking simulation suggested that the isomer can have a high affinity for the EGFR with L858R/T790M double mutations.

Therefore, in this study, we aimed to synthesize and investigate the potential of an iodinated rociletinib isomer as an imaging agent for EGFR with L858R/T790M double mutations.

Herein, an iodinated rociletinib modified at the trifluoromethyl zone, *N*-{3-[(4-{[4-(4-acetylpiperazin-1-yl)-2-methoxyphenyl]amino}-5-(trifluoromethyl) pyrimidine-2-yl)amino]-5-iodophenyl}acrylamide (I-RMFZ, **10**), was synthesized (Fig. 2), and its activity was evaluated using three kinds of human NSCLC cell lines, namely H1975 (double mutations EGFR L858R/T790M), H3255 (active mutant EGFR L858R), and H441 (wild-type EGFR), in a preliminary study.

MATERIAL AND METHODS

Chemicals

Nacalai Tesque, Inc. (Kyoto, Japan), Merck (Darmstadt, Germany), Fujifilm Wako Pure Chemical Corporation (Osaka, Japan), Kanto Chemical, Co., Inc. (Tokyo, Japan), and Tokyo Chemical Industry, Co., Ltd. (Tokyo, Japan) supplied all solvents and reagents. Nacalai Tesque, Inc. (Kyoto, Japan) provided Dulbecco's modified eagle medium (DMEM)/Ham's F-12 medium, RPMI-1640 medium, 0.25% trypsin-ethylenediaminetetraacetic acid (EDTA), phosphate-buffered saline (PBS), penicillin-streptomycin (PS), while Biowest (Nuaillé, France) provided fetal bovine serum (FBS).

Cell lines

The WST-8 test assessed the half inhibitory concentration (IC_{50}) of I-RMFZ, rociletinib, and gefitinib against three NSCLC cell lines. The cell lines were generously supplied by Dr. Juri G. Gelovani, previously of the Department of Experimental Diagnostic Imaging at the University of Texas MD Anderson Cancer Center in Houston, TX, USA. H1975 (2.5×10^3 cells/well), H3255 (10^4 cells/well), and H441 (2.5×10^3 cells/well) were seeded in 96-well culture plates and cultured in medium supplemented with 10% FBS and 100 IU/mL PS at 37°C, 5% CO_2, and 5% humidity.

Instrumentations

The radioactivity was measured using the Auto Gamma System ARC-7010B (Hitachi Ltd., Tokyo, Japan). The reactions were monitored using thin-layer chromatography (TLC) on silica plates 60 F254 (Merck). The SPD-20A system (Shimadzu Corp., Kyoto, Japan) was used for high-performance liquid chromatography (HPLC). JNM-ECS 400 and JNM-ECA 600 nuclear magnetic resonance (NMR) spectroscopy (JEOL Ltd., Tokyo, Japan) were used. The JMS-T100TD (JEOL Ltd.) was used for direct analysis in real-time mass spectrometry (DART-MS). The JMS-T700 (JEOL Ltd.) was used to perform fast atom bombardment mass spectrometry (FAB-MS). The absorbance in 2-(2-methoxy-4-nitrophenyl)-3-(4-nitrophenyl) -5-(2,4-disulfophenyl)-2H tetrazolium monosodium salt (WST-8) assay was determined using Infinite® F200 Pro microplate reader (TECAN, Switzerland).

Molecular docking

In this current study, molecular docking was performed using the AutoDock Vina package to estimate the interaction in the ligand-receptor complex (Trott and Olson, 2010). The ligand molecule of rociletinib was retrieved from the PubChem database. The structure of ligand was downloaded and saved to an sdf extension. Meanwhile, a structure of I-RMFZ was generated using MarvinSketch program packages. The structure of rociletinib and I-RMFZ were converted to a three-dimensional (3D) structure and saved to a protein data bank (PDB) file. Then, Open Babel 2.4.1 program packages were used to convert the sdf and PDB files into pdbqt formats (O'Boyle et al., 2011). During receptor preparation, the 3D structure of EGFR L858R/T790M was obtained from the RCSB database (PDB ID: 3IKA). The polar hydrogen and Kollman's united atom charges were computed to the receptor. The receptor was saved in pdbqt format. All the docking results were processed and visualized using the Open-Source PyMOL v 2.3 software (Delano, 2020).

The grid box parameter was required to limit the position and conformation of the ligand around the receptor site. The grid box was set at $24 \times 22 \times 22$ with a grid spacing of 1.00 Å. Meanwhile, the grid box center was assigned at the coordinates $-3.764 \times 21.197 \times 30.443$. The exhaustiveness factor was set at 100. Other parameters were calculated using AutoDock Vina's defaults. The search parameter used the Broyden−Fletcher−Goldfarb−Shanno (BFGS) algorithm. Morris et al. built AutoDock Tools 1.5.6, which was used to configure all parameters (Morris et al., 2009). The docking parameters were computed according to similar protocols employed in our previous studies (Arwansyah et al., 2021; Fawwaz et al., 2024; Sumaryada et al., 2016). The simulations obtained were then visualized using the PLIP webserver and PyMOL software version 2.3. The docking output in the form of a protein-ligand complex with the pdbqt format was converted to PDB using AutoDock Tools 1.5.6. The PDB file was submitted to the PLIP webserver (https://plip-tool.biotec.tu-dresden.de/plip-web/plip/index) to study the protein−ligand interactions. Furthermore, the pse format generated on the web server was saved and encoded into the PyMOL

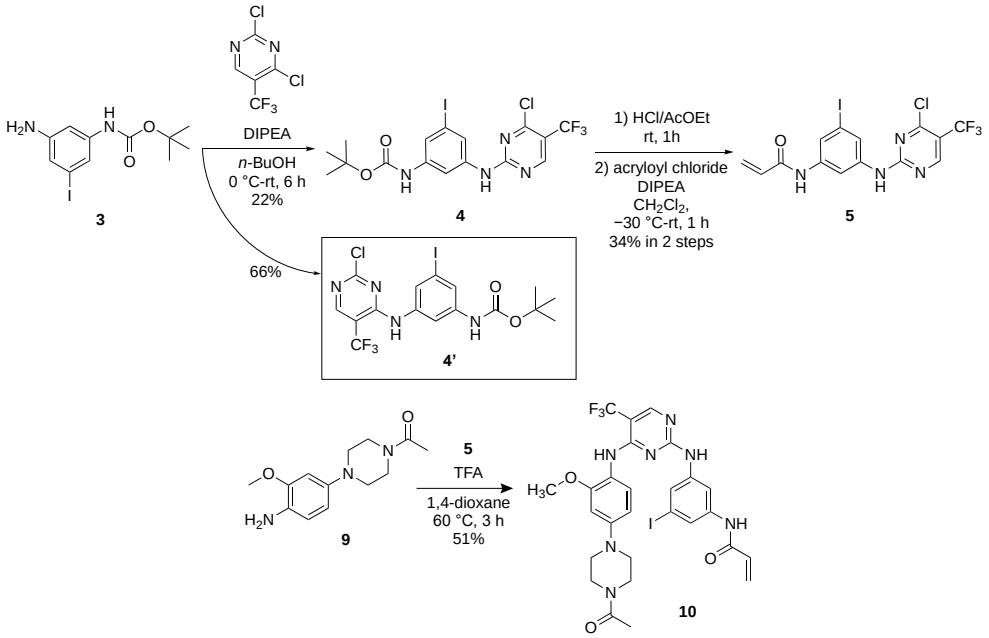

Figure 2. The synthetic procedure of iodinated rociletinib analog (I-RMFZ, **10**).

software to visualize the protein-ligand complex interactions.

Probe synthesis

I-RMFZ was synthesized according to our previous study (Fawwaz et al., 2020), as shown in Fig. 2.

*Synthesis of compound **4***

Compound **4** was synthesized according to the methods employed in our previous study, but with a slight modification (Fawwaz et al., 2020). Isomers were produced during the synthesis of compound 4. These isomers were separated using HPLC with a recycling system (mobile phase: dichloromethane/methanol = 50/1). The crude product was dissolved in the mobile phase and then injected into the HPLC system with Cosmosil® 5SL-II (20 ID × 250 mm) column at a 9.5 mL/min flow rate. The HPLC purification afforded major isomer (compound 4') and minor isomer (compound **4**) with 66% (0.29 g) (Fawwaz et al., 2020) and 22% (0.10 g) yield, respectively, as a colorless solid. ^{1}H NMR (400 MHz, $CDCl_3$): δ 1.53 (9H, s), 6.66 (1H, s), 7.47 (1H, s), 7.67 (1H, s), 7.71 (1H, S), 7.87 (1H, s), 8.62 (1H, s). ^{13}C NMR (100 MHz, $CDCl_3$): δ 160.1, 157.3, 152.4, 140.0, 139.1, 123.8, 123.3, 122.9, 121.1, 114.0 (CF_3), 109.4, 94.1, 81.3, 28.5 (Fig. 3). HRMS (FAB+) calced for $C_{16}H_{15}ClF_3IN_4O_2$ $[M+H]^+$: *m/z* = 513.9880, found 513.9849.

*Synthesis of compound **5***

Compound **5** was synthesized according to the methods employed in our previous study, but with a slight modification (Fawwaz et al., 2020). ^{1}H NMR (400 MHz, $(CD_3)_2SO$): δ 5.79 (1H, dd, *J* = 2.4, 10.0 Hz), 6.25 (1H, dd, *J* = 2.0, 16.8 Hz), 6.43 (1H, dd, *J* = 10.4, 17.6 Hz), 7.89 (1H, t, *J* = 2.0 Hz), 7.95–7.93 (2H, m), 8.85 (1H, s), 10.28 (1H, s), 10.77 (1H, s). ^{13}C NMR (100 MHz, $(CD_3)_2SO$): δ 163.5, 160.5, 158.3, 157.9, 140.7, 140.2, 131.7, 127.7, 123.9, 123.2, 122.1, 111.9 (CF_3), 110.8, 94.4 (Fig. 4). HRMS (FAB+) calced for $C_{14}H_9ClF_3IN_4O$ $[M+H]^+$: *m/z* = 467.9462, found 467.9449.

*Synthesis of compound **10***

Compound **10** was synthesized according to the methods employed in our previous study, but with a slight modification (Fawwaz et al., 2020). ^{1}H NMR (400 MHz, $(CD_3)_2SO$): δ 2.04 (3H, s), 3.01 (2H, s), 3.07 (2H, s), 3.56 (4H, q, *J* = 5.2 Hz), 3.79 (3H, s), 5.79 (1H, dd, *J* = 1.6, 6.8 Hz), 6.25-6.31 (2H, m), 6.41 (1H, dd, *J* = 6.8, 11.2 Hz), 6.61 (1H, d, *J* = 1.6 Hz), 7.51 (1H, s), 7.52 (1H, d, *J* = 6 Hz), 8.02 (1H, s), 8.13 (1H, s), 8.31 (1H, s), 10.22 (1H, s) (Fig. 5). HRMS (FAB+) calced for $C_{27}H_{27}F_3IN_7O_3$ $[M+H]^+$: *m/z* = 681.1172, found 681.1166.

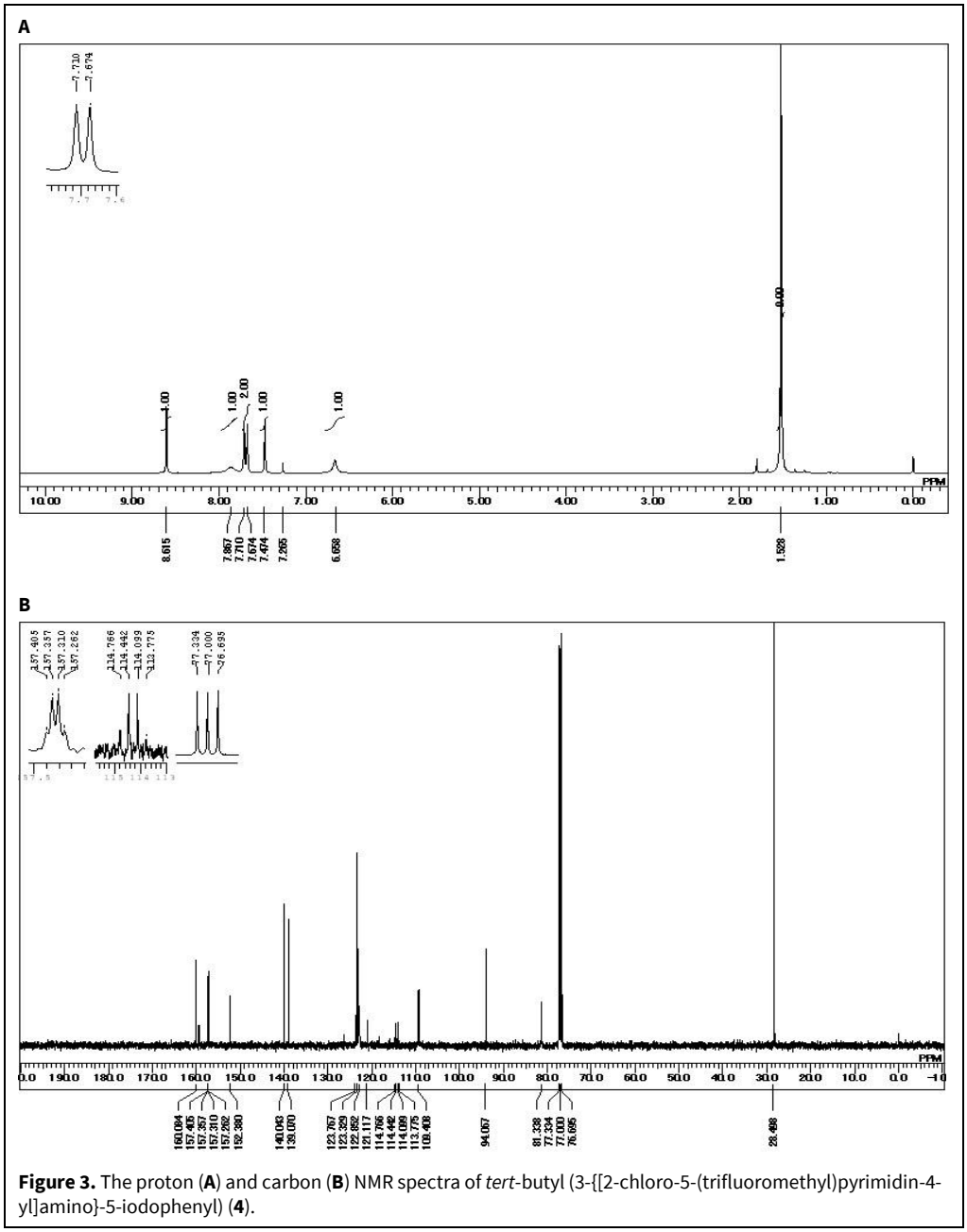

Figure 3. The proton (**A**) and carbon (**B**) NMR spectra of *tert*-butyl (3-{[2-chloro-5-(trifluoromethyl)pyrimidin-4-yl]amino}-5-iodophenyl) (**4**).

Cytotoxicity assay

In 96-well culture plates, the cells were seeded in a mixture supplemented with 10% FBS and 100 IU/mL PS. The cells were allowed to reach a density of 2.5 × 10^3 cells/well (H1975 and H441) and 1 × 10^4 cells/well (H3255) after 24 h of incubation at 37°C at 5% CO_2, and 5% humidity. After 48 h of treatment with various doses (0.01–100 μM) of I-RMFZ, the IC_{50} was determined using Cell Counting Kit-8 (Dojindo, Kumamoto, Japan), according to the manufacturer's instructions (Fawwaz et al., 2020). The selectivity index (SI) was calculated as the ratio of the IC_{50} value in H1975 cells to the IC_{50} value in H441 cells (Céspedes et al., 2023).

Statistical analysis

The significance between I-RMFZ and rociletinib for cytotoxicity assay was statistically analyzed by unpaired Student's *t*-test using GraphPad Prism 8.4.3 software (GraphPad Software, San Diego, CA, USA). All values were presented as mean ± standard deviation (SD), and $p<0.05$ was considered statistically significant.

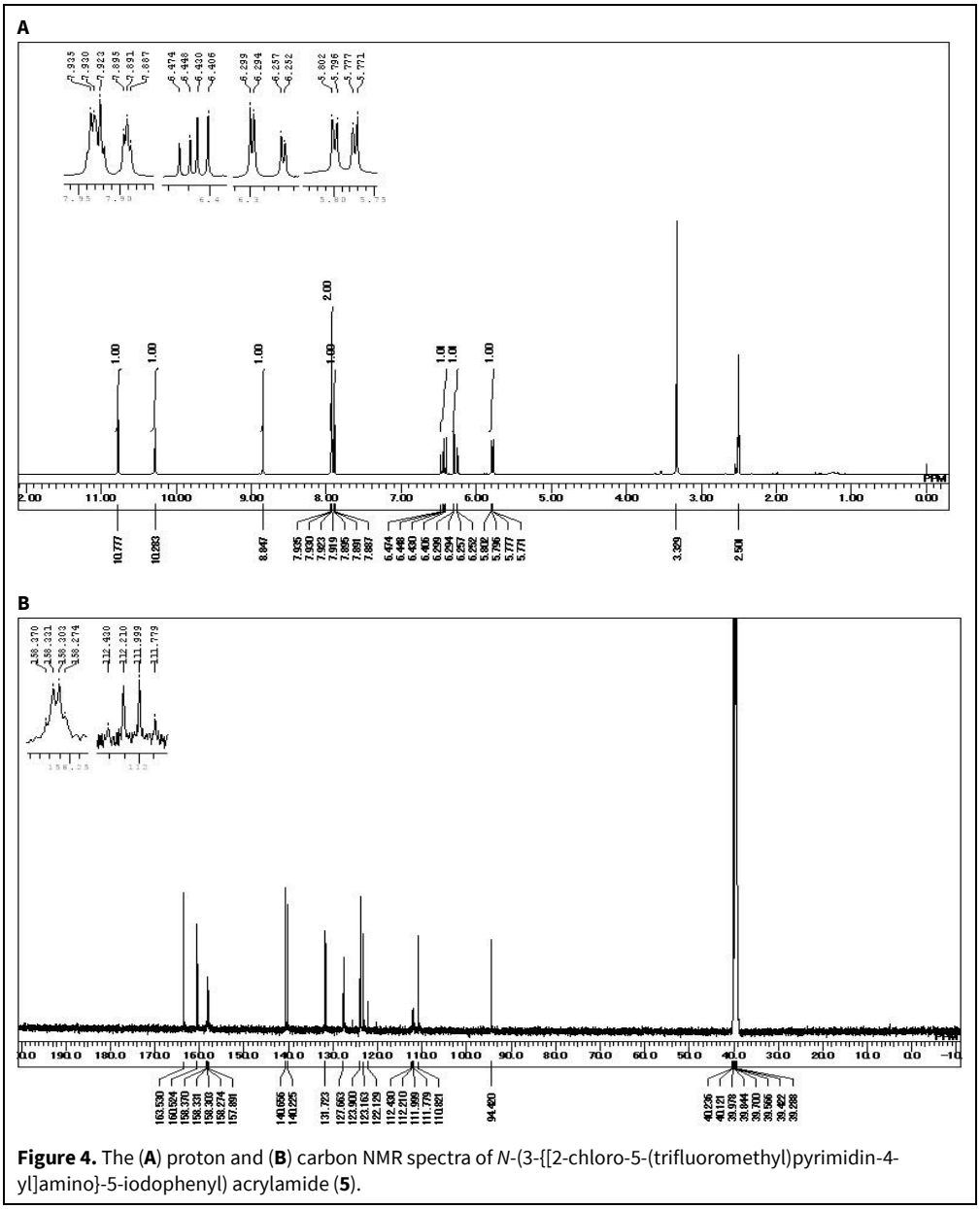

Figure 4. The (**A**) proton and (**B**) carbon NMR spectra of *N*-(3-{[2-chloro-5-(trifluoromethyl)pyrimidin-4-yl]amino}-5-iodophenyl) acrylamide (**5**).

RESULTS

Molecular docking

The binding mechanism of rociletinib and I-RMFZ to the active site of EGFR L858R/T790M was investigated using a molecular docking simulation (PDB code: 3IKA). This URL, http://vina.scripps.edu/tutorial.html (accessed September 25, 2023), includes a comprehensive description of the AutoDock Vina docking tutorials and fundamental principles. The binding energy of rociletinib and I-RMFZ associated with EGFR L858R/T790M was estimated at −7.6 and −7.4 kcal/mol, respectively. Tables 1 and 2 summarize the ligand–receptor interactions mediated by hydrogen bonds and hydrophobic interactions, respectively. The binding position of ligands at the receptor site is depicted in Fig. 6.

Probe synthesis

The non-radioactive iodinated I-RMFZ, a rociletinib analog, was synthesized using 5-iodo-*m*-phenylenediamine instead of *m*-phenylenediamine in the described production technique (Fawwaz et al., 2020) (Fig. 2). Iodine was added to the diaminophenyl group of rociletinib because a molecular docking study demonstrated that iodine in this position does not affect the affinity of I-RMFZ for EGFR L858R/T790M. The anilinopyrimidine core and trifluoromethyl groups are the most significant substituents that help rociletinib bind to EGFR L858R/T790M, according to their complex crystal structure (Yan et al., 2017).

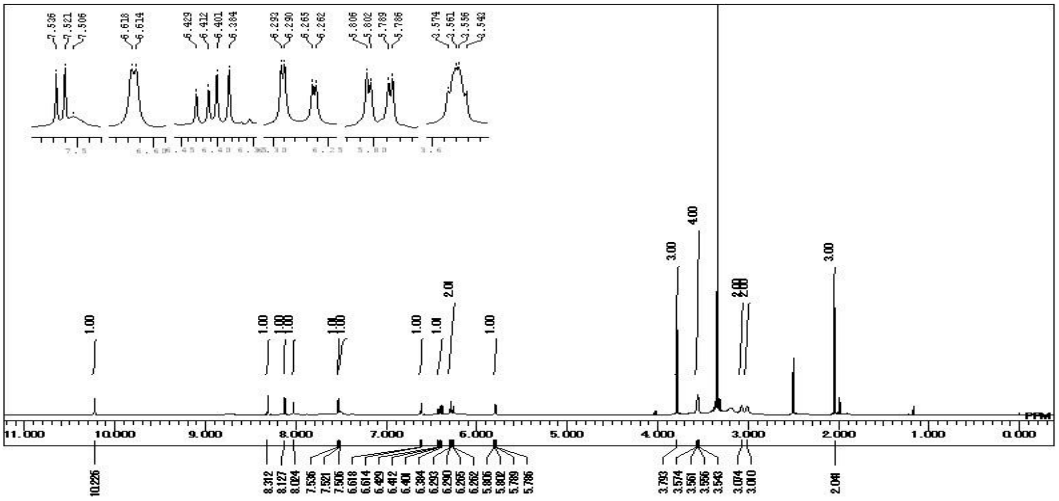

Figure 5. The proton NMR spectrum of *N*-{3-[(4-{[4-(4-acetylpiperazin-1-yl)-2-methoxyphenyl]amino}-5-(trifluoromethyl)pyrimidin-2-yl)amino]-5-iodophenyl}acrylamide (I-RMFZ, **10**).

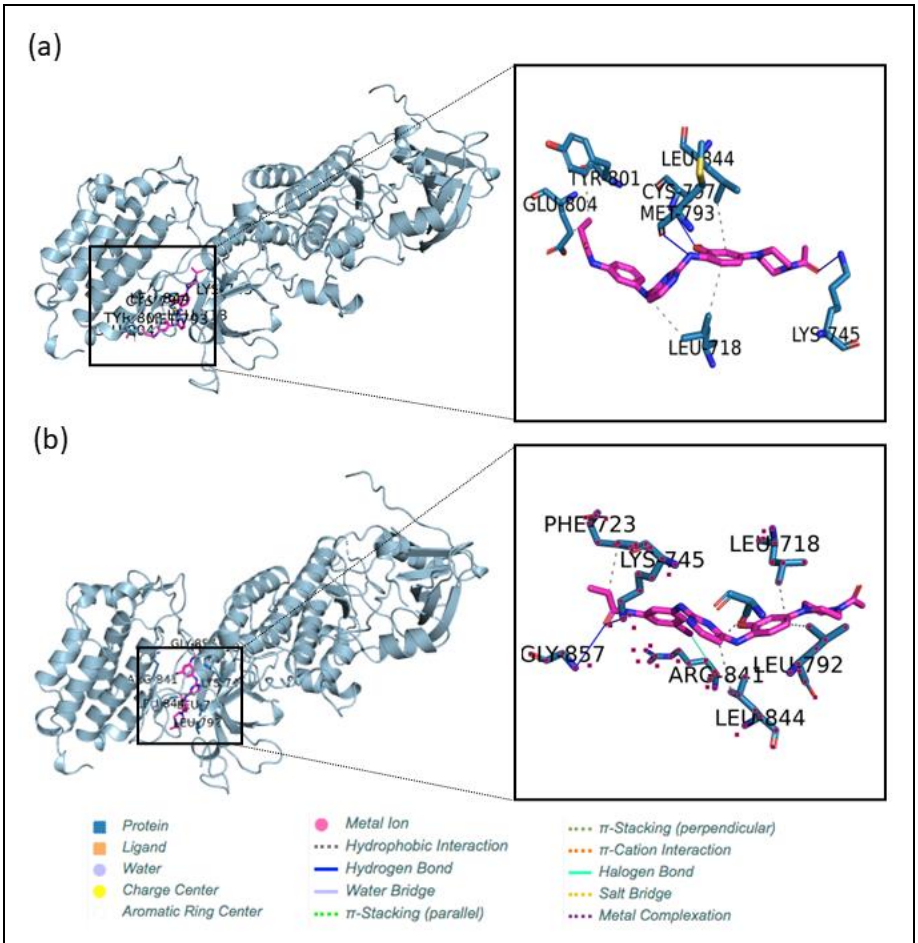

Figure 6. The conformations are assumed by ligands **(a)** rociletinib, **(b)** I-RMFZ and receptor during binding.

Table 1. Hydrogen bonds of ligands in complex with the receptor.

Compound	Residue	AA	Distance H-A (Å)	Distance D-A (Å)	Donor angle	Donor atom	Acceptor atom
Rociletinib	745A	LYS	2.2	3.14	153	470 [N3+]	6014 [O2]
	793A	MET	3.21	3.72	114.35	5998 [Npl]	904 [O2]
	797A	CYS	2.83	3.36	112.65	933 [Nam]	6005 [O3]
I-RMFZ	745A	LYS	2.6	3.04	105.85	470 [N3+]	6030 [O2]
	857A	GLY	3.15	3.76	119.84	1548 [Nam]	6030 [O2]

Table 2. Hydrophobic interactions of ligands in complex with a receptor.

Compound	Residue	AA	Distance	Ligand atom	Protein atom
Rociletinib	718A	LEU	3.67	6004	230
	718A	LEU	3.57	5996	231
	801A	TYR	3.68	6031	974
	804A	GLU	3.82	6031	1012
	844A	LEU	3.93	6001	1432
I-RMFZ	718A	LEU	3.3	6005	230
	723A	PHE	3.66	6031	263
	743A	ALA	3.95	5992	451
	792A	LEU	3.94	6005	898
	844A	LEU	3.99	5992	1431

Table 3. The IC_{50} after exposure of I-RMFZ, rociletinib or gefitinib to NSCLC cell lines by WST-8 assay.

Cell lines	Mutation status	IC_{50} (μM)		
		I-RMFZ	Rociletinib (Fawwaz et al., 2020)	Gefitinib (Fawwaz et al., 2020)
H1975	L858R/T790M	0.10 ± 0.08	0.14 ± 0.05	>10
H3255	L858R	0.24 ± 0.14	0.15 ± 0.02	0.02 ± 0.02
H441	Wild-type	>10	0.26 ± 0.04	>10
Selectivity Index (SI) toward H1975		SI > 100	SI = 1.86	

Data represent the mean ± SD of three separate experiments.

Cytotoxicity assays

IC_{50} of I-RMFZ was determined using WST-8 assay. The cytotoxicity of I-RMFZ against H1975 was similar to that of rociletinib. As demonstrated in Table 3, I-RMFZ is preferred to rociletinib for dual mutations EGFR cell lines. The selectivity of I-RMFZ towards EGFR double mutation compared to wild-type is reflected in the SI value. A trend of cell death over I-RMFZ can also be seen in Fig. 7. The graph shows the potential for apoptosis of I-RMFZ in H1975 and H3255 compared to H441.

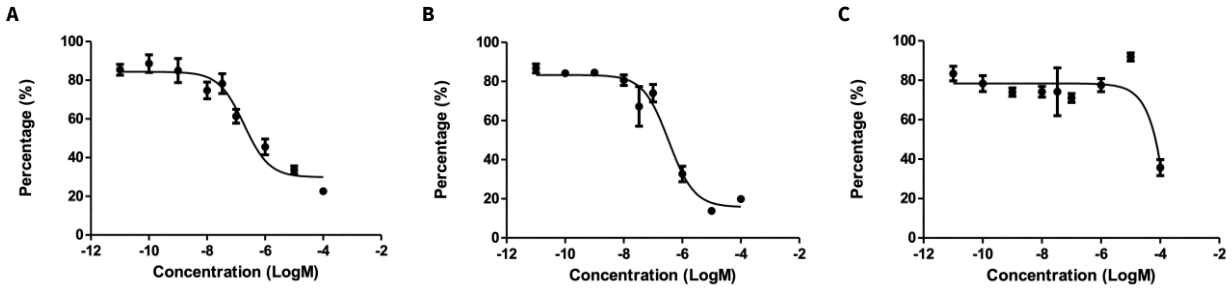

Figure 7. Trend of cell death over I-RMFZ toward NSCLC cell lines **(A)** H1975, **(B)** H3255 and **(C)** H441.

DISCUSSION

Several radiolabeled EGFR TKIs have been developed to serve as imaging agents for estimating the therapeutic effects of TKI therapy on NSCLC. Certain groups have developed promising radiolabeled probes targeting EGFR with L858R or del19 mutation (Gelovani, 2008; Yeh et al., 2011). However, most agents showed unsatisfactory results when stratifying patients with NSCLC of EGFR L858R/T790M double mutations. Therefore, researchers have continued their studies intended to develop an effective imaging agent for diagnosing and stratifying patients with NSCLC with EGFR L858R/T790M double mutations (Fawwaz et al., 2020; 2021; Mishiro et al., 2022; Yeh et al., 2011).

The third-generation TKIs were designed to overcome the limitations of the previous generations by blocking the mutant irreversibly. Several studies have demonstrated that rociletinib selectively inhibits EGFR with mutation, particularly L858R/T790M double mutations (Yan et al., 2017). Due to its selectivity, rociletinib has fewer adverse effects, such as gastrointestinal toxicity, than first-generation and second-generation TKIs (Yan et al., 2017). Given the high selectivity of rociletinib, we designed and synthesized a radioiodinated variant of rociletinib (ICO1686) as an imaging agent. During the research, we obtained an isomer of a synthetic intermediate for ICO1686 synthesis. Using this isomer, we designed and synthesized an ICO1686 analog (I-RMFZ) and evaluated its potential as an imaging agent for EGFR.

I-RMFZ was synthesized through multistep reactions starting from *tert*-butyl(3-{[2-chloro-5-(trifluoromethyl)pyrimidin-4-yl]amino}-5-iodophenyl) carbamate (**4**) which was obtained as a side product in the synthesis of compound **4'**, a synthetic intermediate for the synthesis of ICO1686. To separate these isomers, HPLC with a recycling system was used. These isomers were identified using NMR. The ^{1}H NMR spectrum of the product obtained via the coupling of compound **4** and amine **9** suggested that the material contained the desired I-RMFZ product as a major component.

Molecular docking investigation suggested that I-RMFZ could interact with the EGFR L858R/T790M mutation with a high binding energy comparable to that of rociletinib. Like numerous EGFR kinase inhibitors, the pyrimidine ring of rociletinib established a hydrogen bond with Met-793 and Cys-797 at the hinge region (Table 1 and Fig. 6). The acrylamide group of I-RMFZ formed two hydrogen bonds with Lys-745 and Gly-857 (Table 2). Moreover, the iodine of I-RMFZ formed a halogen bond with Arg-841. Further, I-RMFZ formed some hydrophobic interactions with EGFR, which can contribute to the affinity of the ligand for the EGFR L858R/T790M.

In vitro, cytotoxicity assay was performed to support molecular docking studies. Similar to rociletinib, I-RMFZ exhibited higher cytotoxicity toward cell lines with EGFR mutations compared to those with wild-type EGFR (Table 3). The cytotoxicity of I-RMFZ against H1975 was higher than that of gefitinib, which does not exhibit cytotoxicity against H1975. These data agree with previous reports on third-generation EGFR TKIs (Yang et al., 2021). In the EGFR kinase domain, the anilinopyrimidine of rociletinib formed hydrogen bonds with the NH and CO in the main chain of Met-793. In addition, Met-790, the mutant residue, can form hydrophobic interactions with the trifluoromethyl substituent of rociletinib (Yan et al., 2017). In contrast, gefitinib suppressed only H3255 cell growth. These data agree with the previous study (Sequist et al., 2015; Yeh et al., 2011). Rociletinib showed cytotoxicity against H441 with IC_{50} 0.26 ± 0.04, while I-RMFZ did not show cytotoxicity against H441. Thus, I-RMFZ was more selective for the EGFR L858R/T790M mutation (SI > 100) than rociletinib was (SI = 1.86). These features suggest that the radioiodinated variant of I-RMFZ can be an imaging agent to determine EGFR mutation status.

Our previous study demonstrated that radioiodinated rociletinib [^{125}I]ICO1686 exhibits remarkable selectivity toward dual mutation EGFR in an *in vitro*

cell uptake study. This result was supported by the kinase assay study, in which [^{125}I]ICO1686 showed higher selectivity (SI > 32) toward EGFR with L858R/T790M double mutations than wild-type EGFR did, which is comparable to that of rociletinib (SI = 42). However, an *in vivo* biodistribution analysis resulted in an insufficient tumor accumulation (Fawwaz et al., 2020). As I-RMFZ exhibits a higher SI toward H1975 than that of previously reported EGFR TKIs, we anticipate that it may accumulate in H1975 tumors more than in other organs and tissues.

CONCLUSION

The isomer of iodinated rociletinib, I-RMFZ, was successfully synthesized through a multistep process. I-RMFZ demonstrated highly selective cytotoxicity toward cell lines with EGFR L858R/T790M mutations. Molecular docking studies supported the high affinity of I-RMFZ toward EGFR with double mutations. Our results indicate that [^{123}/^{124}I]I-RMFZ, the radioiodinated variant of I-RMFZ, can be used for imaging of EGFR L858R/T790M double mutations.

CONFLICT OF INTEREST

The authors declare no conflicts of interest.

ACKNOWLEDGMENTS

This work was supported by Terumo Life Science Foundation and MEXT KAKENHI Grant-in-Aid for Scientific Research (16H05397) and the Ministry of Research, Technology and Higher Education, Indonesia. The authors greatly acknowledge the Gadjah Mada University Research Directorate and Gadjah Mada University Reputation Enhancement Team Towards World Class University.

REFERENCES

Ariyama T, Kanno Y, Takizawa S, Nemoto K, Ishii T (2021) Comparative study of different epidermal growth factor receptor (EGFR)-tyrosine kinase inhibitors affecting lung cancer cell lines stably overexpressing EGFR mutations. BPB Rep 4: 12–16. https://doi.org/10.1248/bpbreports.4.1_12

Arwansyah A, Arif AR, Syahputra G, Sukarti S, Kurniawan I (2021) Theoretical studies of thiazolyl-pyrazoline derivatives as promising drugs against malaria by QSAR modelling combined with molecular docking and molecular dynamics simulation. Mol Simul 47: 988–1001. https://doi.org/10.1080/08927022.2021.1935926

Ballard P, Yates JWT, Yang Z, Kim D-W, Yang JC-H, Cantarini M, Pickup K, Jordan A, Hickey M, Grist M (2016) Preclinical comparison of osimertinib with other EGFR-TKIs in EGFR-mutant NSCLC brain metastases models, and early evidence of clinical brain metastases activity. Clin Cancer Res 22: 5130–5140. https://doi.org/10.1158/1078-0432.Ccr-16-0399

Cavina L, van der Born D, Klaren PHM, Feiters MC, Boerman OC, Rutjes F (2017) Design of radioiodinated pharmaceuticals: Structural features affecting metabolic stability towards *in vivo* deiodination. Eur J Org Chem 2017: 3387–3414. https://doi.org/10.1002/ejoc.201601638

Céspedes I, Fuentes-León F, Rodeiro I, Laurencio-Lorca Y, Iglesias M, Herrera J, Cuellar C, Caballero V, Pereira L, Cuétara E, Sánchez A, Fernández M, Núñez R, Hernández-Balmaseda I, Ortiz E (2023). Kinetic characterization, antioxidant and *in vitro* toxicity potential evaluation of the extract M116 from *Bacillus amyloliquefaciens*, a Cuban southern coast marine microorganism. J Pharm Pharmacogn Res 11: 547-556. https://doi.org/10.56499/jppres23.1574_11.4.547

Delano DL: The PyMOL Molecular Graphics System, Version 2.3. (2020) In Book The PyMOL Molecular Graphics System, Version 2.3. (2020) (Editor ed.eds.). pp. https://pymol.org/. City; 2020: https://pymol.org/

Dubost E, McErlain H, Babin V, Sutherland A, Cailly T (2020) Recent advances in synthetic methods for radioiodination. J Org Chem 85: 8300–8310. https://doi.org/10.1021/acs.joc.0c00644

Fawwaz M, Mishiro K, Nishii R, Sawazaki I, Shiba K, Kinuya S, Ogawa K (2020) Synthesis and fundamental evaluation of radioiodinated rociletinib (CO-1686) as a probe to lung cancer with L858R/T790M mutations of epidermal growth factor receptor (EGFR). Molecules 25: 2914. https://doi.org/10.3390/molecules25122914

Fawwaz M, Mishiro K, Nishii R, Makino A, Kiyono Y, Shiba K, Kinuya S, Ogawa K (2021) A radiobrominated tyrosine kinase inhibitor for EGFR with L858R/T790M mutations in lung carcinoma. Pharmaceuticals (Basel) 14: 256. https://doi.org/10.3390/ph14030256

Fawwaz M, Mishiro K, Arwansyah A, Nishii R, Ogawa K (2024) Synthesis and initial *in vitro* evaluation of olmutinib derivatives as prospective imaging probe for non-small cell lung cancer. Bioimpacts 14: 27774. https://doi.org/10.34172/bi.2023.27774

Fawwaz M, Pratama M, Aminuddin AH, Baits M (2023) Radiolabeled EGFR tyrosine kinase for the detection of dual mutations EGFR L858R/T790M in NSCLC. Biointerface Res Appl Chem 13: 500.

Gelovani JG (2008) Molecular imaging of epidermal growth factor receptor expression-activity at the kinase level in tumors with positron emission tomography. Cancer Metastasis Rev 27: 645–653. https://doi.org/10.1007/s10555-008-9156-5

Hirsch FR, Varella-Garcia M, Bunn PA, Di Maria MV, Veve R, Bremnes RM, Barón AE, Zeng C, Franklin WA (2003) Epidermal growth factor receptor in non–small-cell lung carcinomas: correlation between gene copy number and protein expression and impact on prognosis. J Clin Oncol 21: 3798–3807. https://doi.org/10.1200/JCO.2003.11.069

Hirsch FR, Varella-Garcia M, McCoy J, West H, Xavier AC, Gumerlock P, Bunn PA, Franklin WA, Crowley J, Gandara DR (2005) Increased epidermal growth factor receptor gene copy number detected by fluorescence in situ hybridization associates with increased sensitivity to gefitinib in patients with bronchioloalveolar carcinoma subtypes: A Southwest Oncology Group Study. J Clin Oncol 23: 6838–6845. https://doi.org/10.1200/JCO.2005.01.2823

Kosaka T, Yatabe Y, Endoh H, Yoshida K, Hida T, Tsuboi M, Tada H, Kuwano H, Mitsudomi T (2006) Analysis of epidermal growth factor receptor gene mutation in patients with non-small cell lung cancer and acquired resistance to gefitinib. Clin Cancer Res 12: 5764–5769. https://doi.org/10.1158/1078-0432.Ccr-06-0714

Lüönd F, Tiede S, Christofori G (2021) Breast cancer as an example of tumour heterogeneity and tumour cell plasticity during malignant progression. Br J Cancer 125: 164–175. https://doi.org/10.1038/s41416-021-01328-7

Manning HC (2015) World Molecular Imaging Congress 2015: precision medicine visualized. Mol Imaging Biol 17: 295–296. https://doi.org/10.1007/s11307-015-0855-3

Mishiro K, Nishii R, Sawazaki I, Sofuku T, Fuchigami T, Sudo H, Effendi N, Makino A, Kiyono Y, Shiba K, Taki J, Kinuya S, Ogawa K (2022) Development of radiohalogenated osimertinib derivatives as imaging probes for companion diagnostics of osimertinib. J Med Chem 65: 1835–1847. https://doi.org/10.1021/acs.jmedchem.1c01211

Morris GM, Huey R, Lindstrom W, Sanner MF, Belew RK, Goodsell DS, Olson AJ (2009) AutoDock4 and AutoDockTools4: Automated docking with selective receptor flexibility. J Comput Chem 30: 2785–2791. https://doi.org/https://doi.org/10.1002/jcc.21256

O'Boyle NM, Banck M, James CA, Morley C, Vandermeersch T, Hutchison GR (2011) Open Babel: An open chemical toolbox. J Cheminform 3: 33. https://doi.org/10.1186/1758-2946-3-33

Ogawa K, Takeda T, Yokokawa M, Yu J, Makino A, Kiyono Y, Shiba K, Kinuya S, Odani A (2018) Comparison of radioiodine- or radiobromine-labeled RGD peptides between direct and indirect labeling methods. Chem Pharm Bull 66: 651–659. https://doi.org/10.1248/cpb.c18-00081

Ogawa K, Shiba K, Akhter N, Yoshimoto M, Washiyama K, Kinuya S, Kawai K, Mori H (2009) Evaluation of radioiodinated vesamicol analogs for sigma receptor imaging in tumor and radionuclide receptor therapy. Cancer Sci 100: 2188–2192. https://doi.org/10.1111/j.1349-7006.2009.01279.x

Park S, Lee SY, Kim D, Sim YS, Ryu J-S, Choi J, Lee SH, Ryu YJ, Lee JH, Chang JH (2021) Comparison of epidermal growth factor receptor tyrosine kinase inhibitors for patients with lung adenocarcinoma harboring different epidermal growth factor receptor mutation types. BMC Cancer 21: 52. https://doi.org/10.1186/s12885-020-07765-6

Patel N, Duffy BA, Badar A, Lythgoe MF, Årstad E (2015) Bimodal imaging of inflammation with SPECT/CT and MRI using iodine-125 labeled VCAM-1 targeting microparticle conjugates. Bioconjugate Chem 26: 1542–1549. https://doi.org/10.1021/acs.bioconjchem.5b00380

Peled N, Roisman LC, Miron B, Pfeffer R, Lanman RB, Ilouze M, Dvir A, Soussan-Gutman L, Barlesi F, Tarcic G (2017) Subclonal therapy by two EGFR TKIs guided by sequential plasma cell-free DNA in EGFR-mutated lung cancer. J Thorac Oncol 12: e81-e84. https://doi.org/10.1016/j.jtho.2017.02.023

Sequist LV, Waltman BA, Dias-Santagata D, Digumarthy S, Turke AB, Fidias P, Bergethon K, Shaw AT, Gettinger S, Cosper AK (2011) Genotypic and histological evolution of lung cancers acquiring resistance to EGFR inhibitors. Sci Transl Med 3: 75ra26. https://doi.org/10.1126/scitranslmed.3002003

Sequist LV, Soria JC, Goldman JW, Wakelee HA, Gadgeel SM, Varga A, Papadimitrakopoulou V, Solomon BJ, Oxnard GR, Dziadziuszko R (2015) Rociletinib in EGFR-mutated non-small-cell lung cancer. N Engl J Med 372: 1700–1709. https://doi.org/10.1056/NEJMoa1413654

Singh M, Jadhav HR (2018) Targeting non-small cell lung cancer with small-molecule EGFR tyrosine kinase inhibitors. Drug Discov Today 23: 745–753. https://doi.org/https://doi.org/10.1016/j.drudis.2017.10.004

Sumaryada T, Arwansyah, Roslia AW, Ambarsari L, Kartono A (2016) Molecular docking simulation of mangostin derivatives and curcuminoid on maltase- glucoamylase target for searching anti-diabetes drug candidates. In 2016 1st International Conference on Biomedical Engineering (IBIOMED), pp. 1–4. https://doi.org/10.1109/IBIOMED.2016.7869832

Sun X, Xiao Z, Chen G, Han Z, Liu Y, Zhang C, Sun Y, Song Y, Wang K, Fang F (2018) A PET imaging approach for determining EGFR mutation status for improved lung cancer patient management. Sci Transl Med 10: eaan8840. https://doi.org/10.1126/scitranslmed.aan8840

Tan DS, Yom SS, Tsao MS, Pass HI, Kelly K, Peled N, Yung RC, Wistuba, II, Yatabe Y, Unger M (2016) The International Association for the Study of Lung Cancer Consensus Statement on Optimizing Management of EGFR Mutation-Positive Non-Small Cell Lung Cancer: Status in 2016. J Thorac Oncol 11: 946–963. https://doi.org/10.1016/j.jtho.2016.05.008

Trott O, Olson AJ (2010) AutoDock Vina: Improving the speed and accuracy of docking with a new scoring function, efficient optimization, and multithreading. J Comput Chem 31: 455–461. https://doi.org/https://doi.org/10.1002/jcc.21334

Waaijer SJH, Kok IC, Eisses B, Schröder CP, Jalving M, Brouwers AH, Lub-de Hooge MN, de Vries EGE (2018) Molecular imaging in cancer drug development. J Nucl Med 59: 726–732. https://doi.org/10.2967/jnumed.116.188045

Walker RA, Dearing SJ (1999) Expression of epidermal growth factor receptor mRNA and protein in primary breast carcinomas. Breast Cancer Res Treat 53: 167–176. https://doi.org/10.1023/A:1006194700667

Xiao Z, Song Y, Kai W, Sun X, Shen B (2017) Evaluation of 99m Tc-HYNIC-MPG as a novel SPECT radiotracer to detect EGFR-activating mutations in NSCLC. Oncotarget 8: 40732–40742. https://doi.org/10.18632/oncotarget.17251

Xu G, Wu H, Xu Y, Zhang Y, Lin F, Baklaushev VP, Chekhonin VP, Peltzer K, Wang X, Mao M (2021) Homogenous and heterogenous prognostic factors for patients with bone sarcoma. Orthop Surg 13: 134–144. https://doi.org/https://doi.org/10.1111/os.12851

Yan XE, Zhu S-J, Liang L, Zhao P, Choi HG, Yun CH (2017) Structural basis of mutant-selectivity and drug-resistance related to CO-1686. Oncotarget 8: 53508–53517. https://doi.org/10.18632/oncotarget.18588

Yang JC, Reckamp KL, Kim YC, Novello S, Smit EF, Lee JS, Su WC, Akerley WL, Blakely CM, Groen HJM, Bazhenova L, Carcereny Costa E, Chiari R, Hsia TC, Golsorkhi T, Despain D, Shih D, Popat S, Wakelee H (2021) Efficacy and safety of rociletinib versus chemotherapy in patients with EGFR-mutated NSCLC: The results of TIGER-3, a phase 3 randomized study. JTO Clin Res Rep 2: 100114. https://doi.org/10.1016/j.jtocrr.2020.100114

Yarden Y, Sliwkowski MX (2001) Untangling the ErbB signalling network. Nat Rev Mol Cell Biol 2: 127–137. https://doi.org/10.1038/35052073

Yarden Y (2001) The EGFR family and its ligands in human cancer: signalling mechanisms and therapeutic opportunities. Eur J Cancer 37: 3–8. https://doi.org/10.1016/S0959-8049(01)00230-1

Yeh HH, Ogawa K, Balatoni J, Mukhapadhyay U, Pal A, Gonzalez-Lepera C, Shavrin A, Soghomonyan S, Flores L 2nd, Young D, Volgin AY, Najjar AM, Krasnykh V, Tong W, Alauddin MM, Gelovani JG (2011) Molecular imaging of active mutant L858R EGF receptor (EGFR) kinase-expressing nonsmall cell lung carcinomas using PET/CT. Proc Natl Acad Sci USA 108: 1603–1608. https://doi.org/10.1073/pnas.1010744108

AUTHOR CONTRIBUTION:

Contribution	Fawwaz M	Mishiro K	Purwono B	Nishii R	Ogawa K
Concepts or ideas				x	x
Design	x	x	x	x	x
Definition of intellectual content	x	x	x	x	x
Literature search	x	x	x		x
Experimental studies	x	x			
Data acquisition	x	x	x		x
Data analysis	x	x	x		x
Statistical analysis	x	x			x
Manuscript preparation	x	x	x	x	x
Manuscript editing	x	x	x	x	x
Manuscript review	x	x	x	x	x

Citation Format: Fawwaz M, Mishiro K, Purwono B, Nishii R, Ogawa K (2024) Synthesis and evaluation of a rociletinib analog as prospective imaging double mutation L858R/T790M in non-small cell lung cancer. J Pharm Pharmacogn Res 12(2): 231–242.
https://doi.org/10.56499/jppres23.1743_12.2.231